Resonance damping of LCL filters via input admittance frequency shaping

Jorge Pérez, Santiago Cóbreces,
Daniel Pizarro, Francisco Javier Rodríguez Sánchez
Departamento de Electrónica
Universidad de Alcalá
Email: jorge.perez@depeca.uah.es

Robert Griñó
Inst. of Industrial and Control Engineering.(IOC)
Universitat Politècnica de Catalunya (UPC)
Email: roberto.grino@upc.edu

***Abstract*—This paper presents a novel active damping technique of current-controlled grid-connected power converters through LCL filters. Based on $\mathcal{H}_\infty$ synthesis algorithms, a grid current controller is obtained so that the grid-connected power converted-based application admittance resembles a given frequency reference. By defining a low resistive admittance as the reference, considered application resonance is effectively damped, reducing grid current oscillations under grid voltage variations and avoiding their associated stability problems. Presented grid current controller senses only the PCC grid voltage and current, and is experimentally tested in both time and frequency domains. Additionally, the effectiveness of presented damping method is proved under different grid impedance scenarios.**

I. Introduction

Pulsewidth modulated (PWM) power electronic converters are usually connected to the grid through input filters in order to ensure low THD sinusoidally shaped grid currents [1]. Regarding grid current control applications, one of the most common topologies is the LCL filter [2], which has better filtering capability than simpler topologies as, for example, the L filter, but also increases control complexity [3]. That is due to the presence of two complex conjugate poles in the controlled plant, which resonantly increases its open-loop gain (i.e., its admittance value).

This resonance will generate current oscillations (at the resonant frequency) under changes in the system operating point (e.g., PCC voltage perturbations). These oscillations can be more or less durable over time and high in magnitude depending on how damped the resonance is. Moreover, they can become unstable in presence of non-dissipative closed-loop systems [4] and weak grids [5].

Damping techniques of resonant systems have received significant attention by the specialized literature. They can be sorted in two big groups; active damping [2], [3], [5]–[10], where the system controller is modified to damp the resonance, and passive damping [1], [11]–[14], where passive elements, commonly resistances, are added to the filter to displace the resonant poles. Passive damping is a simpler solution but comes at the cost of extra power loss and reduction of the high-frequency attenuation capability [13]. Active damping techniques overcome passive damping drawbacks, but its effectiveness, however, is limited by the switching frequency,

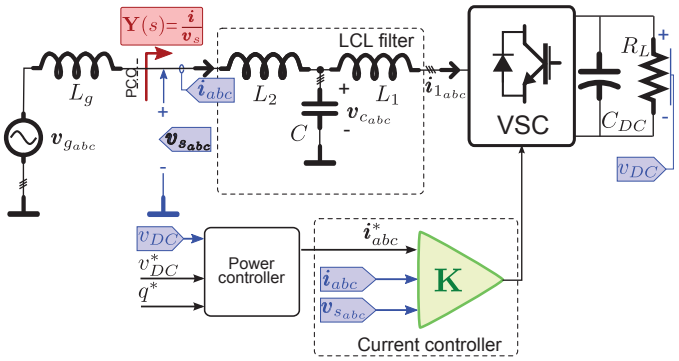

Fig. 1. One-line equivalent diagram of the considered system. In blue the measured variables, in green the current controller and in red the input admittance to be shaped.

and additional passive components may still be needed to damp high-frequency resonance [11].

This paper proposes a new active damping technique for grid-connected power electronic converters through LCL filters by directly shaping, in the frequency domain, the closed-loop input admittance of the considered application. A model-reference approach is adopted, where designer defines the desired admittance at the resonant frequency and an $\mathcal{H}_\infty$ synthesis algorithm obtain the (sub)optimal controller that makes the closed-loop input admittance match the given reference [17]. The system resonance will be effectively damped, then, by defining a purely resistive admittance as the reference.

The rest of the paper is organized as follows. Section II models the plant of the considered application and introduce the resonant behaviour of the LCL filter. Section III develop the proposed system control, starting with the controller objectives and ending up with its design. Section IV discuss the results of the proposed controller, experimentally tested in both time and frequency domains. Additionally, it shows how robust the controller is, regarding both stand-alone stability and damping capability under different grid conditions. The paper ends with a brief discussion of its conclusions.

II. Dynamic modelling

This paper considers a grid current control of a shunt converter connected to the grid through an LCL filter (see

Fig. 1). The system is modelled in stationary (i.e., $\alpha\beta$) reference frame, which allows effective controller operation even under unbalanced conditions. Additionally, as $\alpha\beta$ axes are uncoupled, the original MIMO control problem is reduced to the control of two identical SISO problems. For the sake of notation simplicity, only one of the controlled channels is considered in this paper for both plant modelling and controller design.

Grid current i dynamic of considered system is represented in the Laplace domain as follows:

$$I(s) = G(s) \cdot U(s) + G_d(s) \cdot V_s(s), \tag{1}$$

where $I(s)$, $U(s)$ and $V_s(s)$ are the grid injected current, the VSC average output voltage and PCC voltage, respectively. Transfer functions $G(s)$ and $G_d(s)$ are the open-loop command-to-output and input open loop admittance, respectively, which will follow the next dynamic expressions if an ideal PCC voltage (i.e., $L_g = 0$) is considered:

$$G(s) = -\frac{Z_c(s)}{Z_{L_1}(s) \cdot Z_c(s) + Z_{L_2}(s) \cdot (Z_{L_1}(s) + Z_c(s))}, \tag{2}$$

$$G_d(s) = \frac{Z_{L_1}(s) + Z_c(s)}{Z_{L_1}(s) \cdot Z_c(s) + Z_{L_2}(s) \cdot (Z_{L_1}(s) + Z_c(s))}, \tag{3}$$

where $Z_c(s) = 1/(sC)$, $Z_{L_1}(s) = sL_1 + R_1$ and $Z_{L_2}(s) = sL_2 + R_2$ are the capacitor, converter-side coil and grid-side coil impedances, respectively.

Both $G(s)$ and $G_d(s)$ have a pair of complex conjugate poles which will produce an increase of their respective gains at the resonance frequency $\omega_{res} = \sqrt{(L_1 + L_2)/(L_1 \cdot L_2 \cdot C)}$ rad/s. Of main importance in the stability of the considered application is the resonance in $G_d(s)$ (refer to Fig. 7 to see its frequency domain representation), as it may cause high current oscillations and even system instability under PCC voltage changes. That problem is increased if the system is connected to a weak grid (i.e., with high grid impedance) [5]. The resonance must be properly damped in order to assure the correct and robust operation of the system.

III. System control

A. Control objectives

The main objective of this paper is the design of a grid current controller that, in addition to track a given reference i^*, can effectively damp the system resonance. In order to do so, this paper proposes the frequency shaping of two closed loop transfer function, tracking transfer function $T(s)$ and closed-loop admittance $Y(s)$, which relate the grid current reference i^* and the PCC voltage v_s to the obtained grid current, respectively.

Fig. 1 shows, in green, the integration of the proposed controller $\mathbf{K}$ in the system. It has three inputs: the measured PCC voltage v_s, the sensed grid current i and its corresponding reference i^*. Even though the controller is obtained as a MIMO system in the synthesis process, is interesting to divide its transfer matrix in rows: $\mathbf{K}(s) = [K_s \quad K_{ref} \quad K_i]^T$. Controller actuation u dynamic can be expressed in the Laplace domain as follows:

$$U(s) = K_s(s) \cdot V_s(s) + K_{ref}(s) \cdot I^*(s) + K_i(s) \cdot I(s). \tag{4}$$

Substituting expressions (4), (2) and (3) in (1) gives the closed loop grid current dynamic in the Laplace domain:

$$I = \underbrace{(1 - GK_i)^{-1} GK_{ref}}_{T(s)} I^* + \underbrace{(1 - GK_i)^{-1} (G_d + GK_s)}_{Y(s)} V_s, \tag{5}$$

where (stand-alone) system stability depends only on the system open-loop transfer function $L = -GK_i$.

The controller design follows a model-reference approach; that is, a controller $\mathbf{K}(s)$ is obtained in order to make the closed-loop transfer functions $Y(s)$ and $T(s)$ resemble two given model references, $Y_{ref}(s)$ and $T_{ref}(s)$. By defining a plain low admittance reference at the system resonance frequency, oscillations can be effectively damped and, as a result, derived stability problems are avoided.

As it is shown in Fig. 1, grid current reference i^* is generated by an outer loop power controller, whose objective may be, for example, maintain the DC-bus voltage v_{DC} equal to a given reference v^*_{DC} even under changes of the load R_L (i.e., the system acts as an active rectifier) [15]. Its design is out of the scope of this work, which is centred in the inner current controller design.

B. Controller design

Controller $\mathbf{K}(s)$ is obtained through an $\mathcal{H}_\infty$ synthesis algorithm, whose input is the generalized plant $\mathbf{P}$ [16]. It is just a virtual MIMO plant with the structure showed below:

$$\begin{bmatrix} \boldsymbol{z} \\ \boldsymbol{v} \end{bmatrix} = \mathbf{P} \begin{bmatrix} \boldsymbol{w} \\ \boldsymbol{u} \end{bmatrix}, \tag{6}$$

where $\boldsymbol{w}$ is called the exogenous inputs vector to the system, $\boldsymbol{z}$ is the *so-called* output error signals, $\boldsymbol{u}$ is the actuation vector that will be computed for the controller and $\boldsymbol{v}$ is the measurements output vector.

$\mathcal{H}_\infty$ synthesis process will compute a (sub)optimal controller $\mathbf{K}$, which minimizes the infinity norm[1] of the closed-loop system $\mathbf{N}$ that results from the feedback interconnection of $\mathbf{P}$ and $\mathbf{K}$, and relates exogenous input vector $\boldsymbol{w}$ and *error vector* $\boldsymbol{z} = \mathbf{N}\boldsymbol{w}$:

$$\min_{\mathbf{K}} \|\mathbf{N}(\mathbf{K})\|_\infty = \min_{\mathbf{K}} \frac{\|\boldsymbol{z}\|_2}{\|\boldsymbol{w}\|_2} \leq \gamma \tag{7}$$

Fig. 2 shows the considered virtual plant $\mathbf{P}$ (in red) used for obtaining the controller $\mathbf{K}$ (in blue) and the resulting closed-loop system $\mathbf{N}$. $\mathbf{P}$ is formed by the open-loop plants G and G_d (in orange) and a set of added elements only necessary for the synthesis process (in purple) which are explained below.

$T_{ref}(s)$ and $Y_{ref}(s)$ are the desired (reference model) tracking and admittance transfer functions. Their outputs, i_t and i_y,

[1]The infinity norm of a MIMO system $\mathbf{H}(s)$ in the frequency domain is defined as $\|\mathbf{H}(s)\|_\infty \triangleq \sup_\omega \bar{\sigma}(\mathbf{H}(j\omega))$, where $\bar{\sigma}(\mathbf{H}(j\omega))$ is the maximum singular value of $\mathbf{H}(j\omega)$. For SISO systems that is simplified to $\|H(s)\|_\infty \triangleq \sup_\omega |H(j\omega)|$

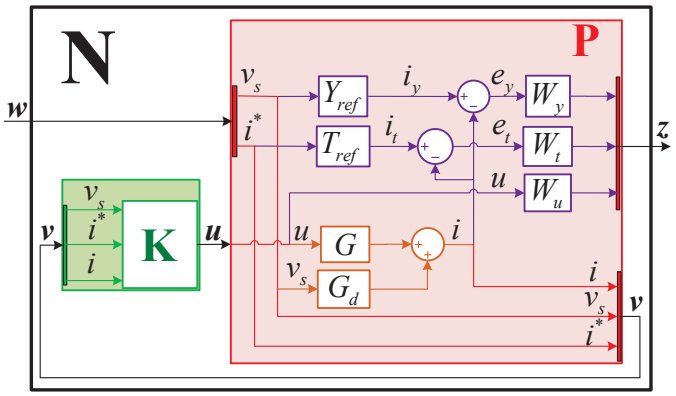

Fig. 2. Structure used for the $\mathcal{H}_\infty$ synthesis. In red the generalized plant $\mathbf{P}(s)$. Wrapped inside of it, in orange the open loop plant $G(s)$ and open loop admittance $G_d(s)$, and in purple the references and weights added for the synthesis. Finally, the obtained controller is represented in green.

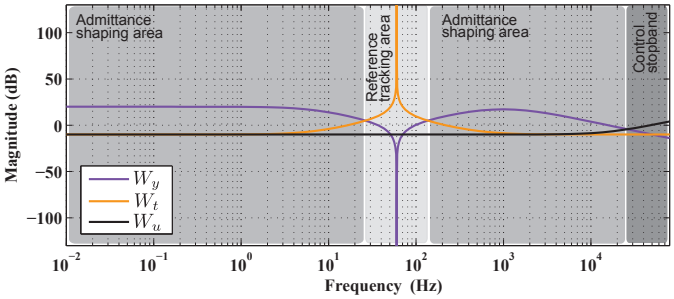

Fig. 3. Magnitude of the selected weights in the frequency domain. The frequency spectrum is divided in areas according to the controller objective in that range.

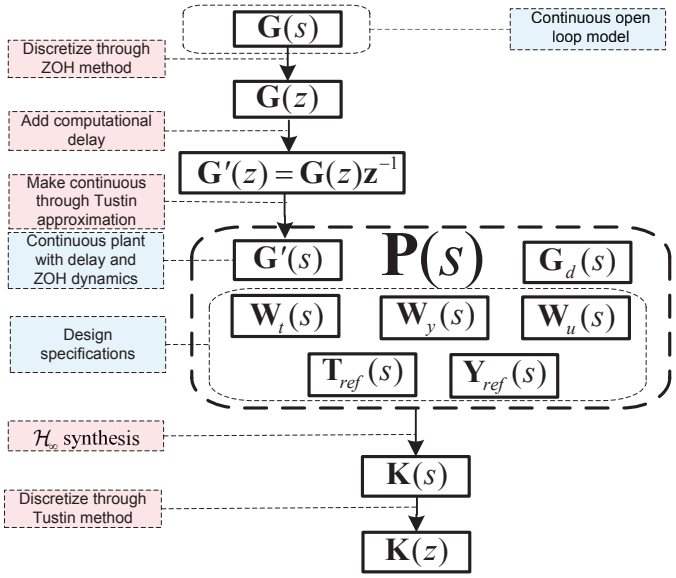

Fig. 4. Flux diagram of the inner controller $\mathbf{K}$ synthesis and discretization process

mark the reference currents due to tracking and admittance control effects, respectively. Grid current i is subtracted from both reference currents, giving two different errors: e_t for tracking and e_y for admittance control. Both controller objectives (i.e., admittance and tracking shaping) can be achieved by means of minimizing these two errors. But, as both errors depend on the grid current, they can not minimized at the same frequencies (i.e., i can not be equal to both i_t and i_y at the same frequency). Additionally, control bandwidth must be limited by means of control effort u minimization. To handle this trade-off, three frequency-weights ($W_t(s)$, $W_y(s)$ and $W_u(s)$ respectively) multiplies each signals. Output and input signal vectors of generalized plant $\mathbf{P}$ defined in Fig. 2 are then:

$$\boldsymbol{z} = \begin{bmatrix} W_t \cdot e_t \\ W_y \cdot e_y \\ W_u \cdot u \end{bmatrix} \quad \boldsymbol{v} = \begin{bmatrix} v_s \\ i^* \\ i \end{bmatrix} \quad \boldsymbol{w} = \begin{bmatrix} v_s \\ i^* \end{bmatrix} \quad \boldsymbol{u} = u \tag{8}$$

As synthesized controller $\mathbf{K}$ should minimize $\boldsymbol{z}$, increasing one weight at a given frequency (while setting the other two relatively low) should result in the minimization of its input at that frequency. Following this design criterion, and given the controller objectives stated in the previous subsection, suitable frequency-weights are represented in Fig. 3. As it is shown, tracking of current reference i^* is only desired at the grid fundamental frequency, 60 Hz in this application, meanwhile admittance shaping is desired, mainly, at super-synchronous frequencies, which is the location of the LCL-filter resonance (a sub-synchronous admittance shaping is also considered to damp possible low frequency grid oscillation). Finally, control bandwidth is limited at high frequencies. Laplace expressions of the selected weights are showed below:

$$W_t(s) = K_t \frac{s^2 + 2\zeta_n \omega_1 s + \omega_1^2}{s^2 + 2\zeta_d \omega_1 s + \omega_1^2}, \tag{9}$$

where K_t is the initial tracking gain, ω_1 is the fundamental frequency in rad/s and ζ_d and ζ_n will define both maximum gain peak and width of the weight resonance;

$$W_y(s) = K_y \frac{s^2 + 2\zeta_d \omega_1 s + \omega_1^2}{s^2 + 2\zeta_n \omega_1 s + \omega_1^2} \cdot \frac{1}{(1/\omega_y)s + 1} \tag{10}$$

where an initial weight $K_y > K_t$ is defined, ζ_d and ζ_n change positions to define a complementary notch to the tracking weight resonance and an additional pole is defined at high frequency ω_y to delimit the admittance shaping region;

$$W_u(s) = K_u \frac{(1/\omega_{u1})s + 1}{(1/\omega_{u2})s + 1}, \tag{11}$$

where a zero in the frequency ω_{u1} will increase the initial low actuation weight K_u, and a pole at very high frequency ω_{u2} is added just to fulfil $\mathcal{H}_\infty$ synthesizing method requirements.

As for the reference model, a tracking reference $T_{ref} = 1$ is set, which will result in perfect current tracking at fundamental frequency (i.e., $I(j\omega_1) \approx I^*(j\omega_1)$), meanwhile a low resistive admittance of $Y_{ref} = 0.1\ \Omega^{-1}$ is considered, which will result in a properly damped LCL resonance.

Synthesized controller $\mathbf{K}(s)$ is obtained in Laplace continuous domain. In order to be implemented in a digital platform,

Fig. 5. Picture of experimental set-up.

TABLE I. EXPERIMENTAL SETUP PARAMETERS

S_n	17.5 kVA	L_1	3.4 mH
V_g	120 V	R_1	28.8 mΩ
ω_1	$2\pi 60$ rads^{-1}	L_2	1.7 mH
V^*_{DC}	700 V	R_2	18.6 mΩ
T_{sw}	400 μs	C	18 μF
T_s	200 μs	C_{DC}	4.7 mF

it must be previously discretized. The discretization process is summed up in Fig. 4. It is important to point out that the obtained controller, and then the close-loop admittance, takes into account the phase lag introduced by both PWM modulation and computational delay. For more information about the discretization process or the admittance and tracking shaping of power converters refer to [17].

IV. Results

Proposed algorithm has been tested in both simulations and an experimental set-up. The latter consist of an AC programmable power supply Pacific SmartSource 345-AMX, emulating the grid, and a 17.5 kVA two-level VSC connected to it through an LCL filter. Passive loads R_L are connected to the DC-side to test the platform under different operating points. Control algorithm is implemented on a Texas Instruments DSP TMS320DSK6713. Table I sums up set-up parameters, where T_s is the sampling period of the control algorithm and T_{sw} is the converter's IGBTs switching period. A picture of the experimental set-up is shown in Fig. 5.

A. Frequency domain results

Fig. 6 shows theoretical tracking transfer function T (obtained following (5)), which is equal to its reference T_{ref} at the fundamental frequency, as was specified in the design process. Fig. 7 shows the admittance shaping results. Theoretical admittance Y is equal to the given reference Y_{ref} at both sub and super-synchronous frequencies as it was specified.

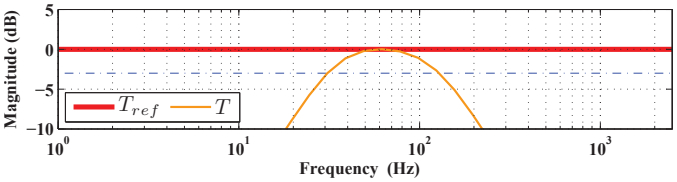

Fig. 6. Obtained tracking transfer function T and its reference T_{ref}.

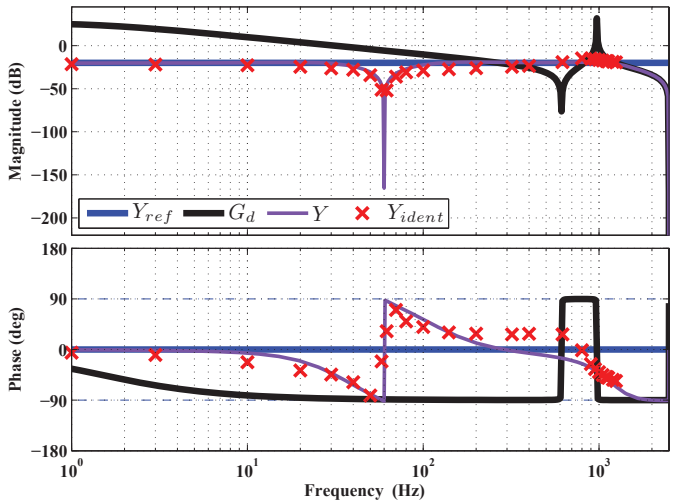

Fig. 7. Admittance frequency results. Open-loop admittance G_d is shown in black. Admittance reference model Y_{ref} is shown on blue color. The closed loop synthesised admittance (theoretical) Y is shown on purple. Red crosses show the experimentally measured admittance Y_{ident}.

Y_{ident} is an experimental admittance measurement obtained by adding a three phase controlled sinusoidal signal to the voltage generated by the AC power supply and analysing, in steady-state, the current response of the converter at that frequency. Of main importance is the resonance frequency of G_d, where more points of Y_{ident} are taken, which proves the good active damping capabilities of the proposed method.

B. System robustness

Fig. 8 shows the obtained system sensitivity function $S = (1 - GK_i)^{-1}$. Its infinity norm $\|S\|_\infty$ is a good inverse indicator of the design stand-alone robustness [16], that is, how much plant parameters may change until the designed system becomes unstable. A commonly design criterion for robust controller is to synthesize loops with $\|S\|_\infty < 6$ dB, which will assure a gain margin bigger than 6 dB and a phase margin bigger than 30°. This criterion is fulfilled, as it can be seen in Fig. 8, which proves the design robustness.

The effects of grid impedance on the presented active damping technique are tested below. Considering a non-ideal inductance L_g at the PCC, the grid current is modified as follows:

$$I(s) = G'(s) \cdot U(s) + G'_d(s) \cdot V_g(s), \qquad (12)$$

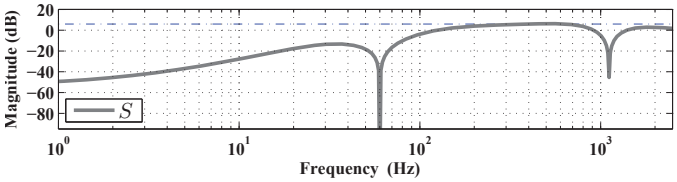

Fig. 8. Obtained sensitivity function S. Blue dash-dotted line marks the accepted 6 dB sensitivity gain limit for robust systems.

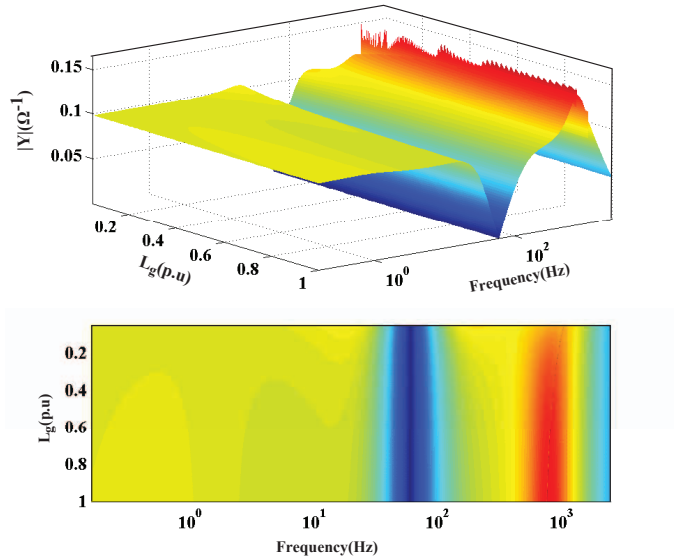

Fig. 9. Effect of modifying the grid inductance L_g on the obtained close loop admittance modulus $|Y'(s)|$.

where $V_g(s) = V_s(s) + (s \cdot L_g) \cdot I(s)$ and

$$G'(s) = -\frac{Z_c(s)}{Z_{L_1}(s) \cdot Z_c(s) + Z_g(s) \cdot (Z_{L_1}(s) + Z_c(s))}, \quad (13)$$

$$G'_d(s) = \frac{Z_{L_1}(s) + Z_c(s)}{Z_{L_1}(s) \cdot Z_c(s) + Z_g(s) \cdot (Z_{L_1}(s) + Z_c(s))} \quad (14)$$

Here $Z_g(s) = s(L_g + L_2) + R_2$ is the new grid-side impedance. Substituting expressions (4), (13) and (14) in (12) gives the new closed loop input admittance $Y'(s)$ seen from the PCC:

$$Y'(s) = \frac{I(s)}{V_s(s)} = \frac{G'(s) \cdot K_s(s) + G'_d(s)}{1 - (G'(s) \cdot K_i(s) + s \cdot L_g \cdot Gd'(s))} \quad (15)$$

Fig. 9 shows closed loop input admittance modulus $|Y'(s)|$ in the frequency domain under changes of the grid inductance $L_g \in [0.05, 1]$ p.u [2]. Presented damping technique is effective even under high grid inductances (i.e., weak grids), as it is shown in the minimum modulus increase over the given admittance reference of 0.1 Ω^{-1}.

C. Time domain results

Fig. 10 shows experimental time domain evolution of the system after the introduction of a DC-load of 4.2 kW. Fig. 11 shows the response of the system under a balanced dip of 60% of the nominal grid voltage value. Both experiments show good current tracking performance. Of main importance is the current response under the grid dip: as can be seen, no oscillation at frequency ω_{res} can be appreciated on it, which proves again the good obtained resonance damping.

[2] L_g is expressed in per unit values of the converter nominal impedance $Z_n = (\sqrt{3}V_g)^2/S_n$.

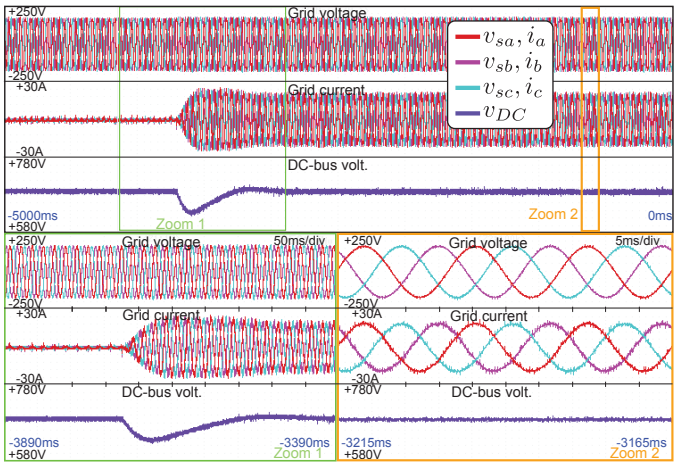

Fig. 10. Connection of a 4.2 kW DC-load with a null reactive reference. Top shows the complete transient. Zoom 1 focuses on the currents and DC-voltage evolution after the connection. Zoom 2 shows grid currents and voltages in steady-state.

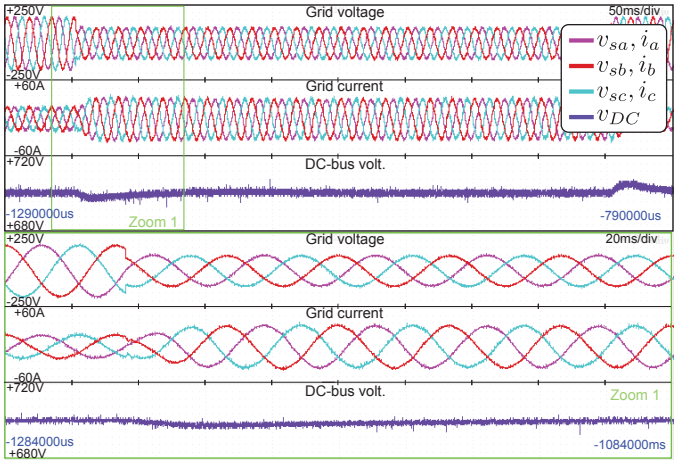

Fig. 11. Response under grid balanced voltage dip when DC-bus is loaded with 4.2 kW. All phases fall to 60% of its value keeping their phase untouched. Top view shows the complete transient in grid voltages, currents and DC-bus voltage. Lower view focuses on the dip initial edge.

V. Conclusion

This work presents a novel active damping technique for current-controlled grid-connected power converters through resonance filters like the LCL. Resonance damping will result in smaller current oscillations under PCC voltage variations and, as a consequence, will improve system stability in connection to weak grids.

Presented active damping technique is based on frequency shaping of the closed-loop input admittance of the considered application, and only needs grid current and grid voltage mea-

surements (i.e., no additional LCL filter sensors are needed). This is achieved by a model-reference approach, where, after designer specifies a desired admittance reference, an $\mathcal{H}_\infty$ synthesis algorithm will obtain the (sub)-optimal controller that shapes the system admittance, in the frequency domain, to follow the given reference. By defining a resistive admittance reference the resonance can be effectively damped, and related stability problems are avoided. Current control design to achieve this goal is explained.

Experimental test of the obtained controller are done and their results are shown. Proposed method shows good current tracking and resonance damping capabilities. The latter is proved experimentally in both frequency and time domains. Moreover, damping technique is demonstrated (theoretically) effective even under extremely high grid impedance, with both good phase and gain margins.

Future works will study the resonance damping and stability robustness under filter and grid modelling uncertainties, and how they are affected by the addition of different control measurements (like filter capacitor voltage or converter side current).

ACKNOWLEDGEMENT

This work of the University of Alcala group was supported in part by the spanish research projects CONPOSITE (ENE2014-57760-C2-2-R Ministerio de Economía y Competitividad) and PRICAM (S2013/ICE-2933 Consejería de educación, juventud y deporte de la Comunidad de Madrid). The work of Robert Griñó was supported in part by the Spanish Research Project DPI2013-41224-P.

REFERENCES

[1] T. Nussbaumer, M. L. Heldwein, and J. W. Kolar, "Differential mode input filter design for a three-phase buck-type pwm rectifier based on modeling of the emc test receiver," *Industrial Electronics, IEEE Transactions on*, vol. 53, no. 5, pp. 1649–1661, 2006.

[2] J. He and Y. W. Li, "Generalized closed-loop control schemes with embedded virtual impedances for voltage source converters with lc or lcl filters," *Power Electronics, IEEE Transactions on*, vol. 27, no. 4, pp. 1850–1861, 2012.

[3] S. G. Parker, B. P. McGrath, and D. G. Holmes, "Regions of active damping control for lcl filters," *Industry Applications, IEEE Transactions on*, vol. 50, no. 1, pp. 424–432, 2014.

[4] L. Harnefors, L. Zhang, and M. Bongiorno, "Frequency-domain passivity-based current controller design," *IET Power Electronics*, vol. 1, no. 4, pp. 455–465, 2008.

[5] M. Liserre, R. Teodorescu, and F. Blaabjerg, "Stability of photovoltaic and wind turbine grid-connected inverters for a large set of grid impedance values," *Power Electronics, IEEE Transactions on*, vol. 21, no. 1, pp. 263–272, 2006.

[6] M. Liserre, A. D. Aquila, and F. Blaabjerg, "Genetic algorithm-based design of the active damping for an lcl-filter three-phase active rectifier," *Power Electronics, IEEE Transactions on*, vol. 19, no. 1, pp. 76–86, 2004.

[7] V. Blasko and V. Kaura, "A novel control to actively damp resonance in input lc filter of a three-phase voltage source converter," *Industry Applications, IEEE Transactions on*, vol. 33, no. 2, pp. 542–550, 1997.

[8] J. L. Agorreta, M. Borrega, J. López, and L. Marroyo, "Modeling and control of-paralleled grid-connected inverters with lcl filter coupled due to grid impedance in pv plants," *Power Electronics, IEEE Transactions on*, vol. 26, no. 3, pp. 770–785, 2011.

[9] J. Dannehl, F. W. Fuchs, S. Hansen, and P. B. Thøgersen, "Investigation of active damping approaches for pi-based current control of grid-connected pulse width modulation converters with lcl filters," *Industry Applications, IEEE Transactions on*, vol. 46, no. 4, pp. 1509–1517, 2010.

[10] Y. Tang, P. C. Loh, P. Wang, F. H. Choo, and F. Gao, "Exploring inherent damping characteristic of lcl-filters for three-phase grid-connected voltage source inverters," *Power Electronics, IEEE Transactions on*, vol. 27, no. 3, pp. 1433–1443, 2012.

[11] M. Cespedes, L. Xing, and J. Sun, "Constant-power load system stabilization by passive damping," *Power Electronics, IEEE Transactions on*, vol. 26, no. 7, pp. 1832–1836, 2011.

[12] R. D. Middlebrook, "Input filter considerations in design and application of switching regulators," *IAS Record, 1976*, 1976.

[13] R. Pena-Alzola, M. Liserre, F. Blaabjerg, R. Sebastián, J. Dannehl, and F. W. Fuchs, "Analysis of the passive damping losses in lcl-filter-based grid converters," *Power Electronics, IEEE Transactions on*, vol. 28, no. 6, pp. 2642–2646, 2013.

[14] R. W. Erickson, "Optimal single resistor damping of input filters," in *Applied Power Electronics Conference and Exposition*, vol. 2. Citeseer, 1999, pp. 1073–1079.

[15] E. J. B. Peña, "Optimización del comportamiento de un convertidor de tres niveles npc conectado a la red eléctrica," Ph.D. dissertation, Politechnic School. University of Alcalá, 2005.

[16] S. Skogestad and I. Postlethwaite, *Multivariable feedback control: analysis and design*. Wiley New York, 2007, vol. 2.

[17] J. Perez, S. Cobreces, F. J. R. Sanchez, and R. Grino, "H-inf simultaneous admittance and tracking current controller of three-phase active grid front-ends," in *Industrial Technology (ICIT), 2015 IEEE International Conference on*. IEEE, 2015, pp. 2092–2097.